International Journal of Remote Sensing and Earth Sciences Vol.11 No.1 June 2014 : 63 – 72

DETECTING THE SPATIAL DISTRIBUTION OF SETTLEMENTS ON VOLCANIC REGION USING IMAGE LANDSAT-8 OLI IMAGERY

Suwarsono*, and M. Rokhis Khomarudin
Remote Sensing Application Center, LAPAN
*e-mail: suwarsono@lapan.go.id

Received: 14 February 2014; Revised: 28 March 2014; Approved: 5 May 2014

Abstract Geologically, Indonesia region is on track ring of fire, brings the consequence that the danger of volcanic eruption could occur at any time. Information sites where the settlement is located in the affected areas on emergency response process is needed in quick time. The availability of up to date data is important because it illustrates the actual condition of the region. Active volcanic landforms ranging from the crater to footslope in general is prone area to volcanic eruption, either by the threat of lava flows, pyroclastic falls, or lahars. This study aims to detect the spatial distribution of the settlement on volcanic region using Landsat-8 OLI. Parameters used for the detection of settlements is Normalized Difference Build-up Index (NDBI). Research methods include radiometric correction, delineation of the boundaries of volcanic landforms, NDBI value extraction, extraction of settlement areas, as well as the accuracy assesment. Study area is Sinabung Volcano region located in the province of North Sumatera. Recently, the volcano experienced a devastating and catastrophic eruption. The results showed that the spatial distribution of settlements on volcanic landforms can be detected quickly from Landsat-8 OLI based on NDBI parameters with a sufficient degree of accuracy.

Keywords : *Settlement, Volcanic Landforms, Sinabung Volcano, NDBI*

1 INTRODUCTION

Detection of settlement areas in the affected area is important to be done to estimate the impact of losses caused by the disaster, both fatalities, number of houses and property. The detection process is most appropriate for the data acquisition period closest to disastrous events as part of the emergency response. In this context, the conditions closest to the disaster event may provide more actual information. Information settlement areas actually can be obtained quickly and efficiently by utilizing remote sensing data.

Volcanic eruption in recent years show an increase in frequency of occurrence. The eruption has caused the disaster that swallowed losses. Some experienced volcanic eruptions in recent years such as Mount Merapi, Soputan, Rokatenda, Lokon, Karangetang, Bur ni Telong, Gamalama, and Sinabung. In early 2014, there was a tremendous explosive eruption of Kelud, which spewed pyroclastic material in which the spread of the volcanic ash reaches the area of Bandung.

Basically, the area on the slopes of the volcano is generally an area with high elevation, steep and dominated by forest land cover. Forests have a vital function, namely the function of conservation, protection functions, and production functions (Act No. 41 of 1999). Although dominated by forest, the slopes of the volcano is also a place to live and strive for humans. One of the main fundamental information required in quick time when the eruption occurred is; locations where settlements are situated on the slopes of volcanoes on the radius of the danger

area. Thus, detection of the locations of settlements in the area of active volcanoes quickly needs to get special attention.

Remote sensing technology offers a method that can be used to detect the settlement areas efficiently, in a relatively fast and with results that can be accounted for accuracy. In remote sensing applications, can be used as well as the Optical SAR data, with different characteristics of spatial, temporal, spectral, and radiometric. Both of these data can be applied for a variety of purposes and interests, which in this study will be directed to the detection of settlement areas on volcanic landforms. In this research will be tested using Landsat-8 OLI is the latest generation of Landsat data which started operation in early 2013.

Satellite Landsat-8 made on the cooperation of the National Aeronautics and Space Administration (NASA) of the United States Geological Survey (USGS) - Department of the Interior (DOI), Orbital Science Corp., Ball Aerospace & Technology Corp., and NASA Goddard Space Flight Center. These satellites Landsat has advantages compared with previous generations, the sensor payload carries. Sensor Landsat-8 consists of a sensor Operational Land Imager (OLI) and the Thermal Infrared Sensor (TIRS). OLI sensor consists of nine spectral channels which have a spatial resolution of 30 m for multispectral channels and 15 m for the panchromatic channel, with a width of 185 km coverage. The width of the spectral range of the sensor OLI is a refinement of ETM + sensor on Landsat satellite 7. This enhancement to avoid the absorption of atmospheric features.

The detection method settlement area in volcanic landform is done digitally by using index variables and undeveloped land (Normalized Difference Build-up Index) or shortened by NDBI. NDBI introduced by Zha *et al.* (2003) for the automation of process mapping and undeveloped land. Model designed NDBI applied to map urban land in Nanjing City, China. Mapping results showed 92.6% accuracy, and show that these parameters can be used to meet reliable mapping. Compared with maximum likelihood classification method, proposed NDBI able to serve as a valuable alternative to rapidly and objectively in the mapping of waking.

In subsequent development, these variables have been used by some researchers to identify land cover, particularly for regions awoke, including settlements using optical data, especially the Landsat data. Jiang *et al.* (2005) used Landsat TM and ETM for analysis of Xi'an city expansion and land cover changes in the surrounding area between 2000 and 2003. The classification method used is the supervised classification with NDBI parameter to restrict urban areas. Ogashawara & Bastos (2012) use NDBI parameter together with parameters NDVI (Normalized Difference Vegetation Index) and NDWI (Normalized Difference Water Index), and its temperature to analyze the relationship between urban land cover and urban heat islands. As-Syakur *et al.* (2012) tries to develop Enhanced parameter Built-Up and Bareness Index (EBBI) on Landsat-7 ETM + as a model to map the area woke up and vacant land with a single calculation. By taking locations in Denpasar Bali, EBBI more effective in distinguishing the undeveloped land and vacant land and further improve the accuracy of the percentage of density and undeveloped land, when compared with the Index-based Built-Up Index (IBI), Normalized Difference Built-up Index (NDBI), Urban Index (UI), Normalized Difference Bareness Index (NDBaI) and Normalized Difference Vegetation Index (NDVI).

Nasipuri & Chatterjee (2009) using the parameter NDBI together with NDVI and NDWI extracted from ASTER data to

determine the condition of land use around Dam Maithon India. NDVI indices used to determine the quality and distribution of vegetation, NDWI to know the characteristics of the waters, and NDBI to determine the distribution and change of open land. In the Middle East region, Uddin *et al.* (2010) tries to discuss the micro-climate variations due to changes in land cover in Kuwait. Landsat period in 1989, 1991 and 2000 are used to calculate the surface temperature and classifying land cover. Land cover classification is done using NDVI parameters, NDWI, NDBI and NDBaI. In these studies also note a positive correlation between the brightness temperature and NDBI.

Xu *et al.* (2013) tries to compare the performance of Landsat-7 ETM + and ASTER to map land up in the southeastern coastal region of China. The study was conducted by comparing three pairs of images by using three approaches, i.e, based on per-band, based on an index-based classification. The index used is the index-based Built-up Index (IBI) and Support Vector Machine (SVM). The results showed that in the study area, the data ETM + and ASTER have a similar performance as a whole in the mapping of open land. IBI values derived from ASTER were consistently higher than those from ETM+.

Chen *et al.* (2006) tries to analyze the relationship between the urban heat island and changes cover/land use in the Pearl River Delta (PRD) using remote sensing data. The data used is Landsat TM and ETM + 1990-2000. In this study, Normalized Difference Bareness Index (NDBaI) is used for the extraction of open land. In the study also examined the relationship between temperature and some indices, NDVI, NDWI and NDBI. Temperatures negatively correlated to the index NDVI, NDWI and NDBaI. While the NDBI, positively correlated temperature. The positive correlation between temperature and brightness and NDBI negative correlation between the brightness temperatures and NDVI is the same as the results of research conducted by Zhang *et al.* (2008).

Furthermore, Zhang *et al.* (2009) sought to know the characteristics of the land surface temperature in catchment areas with impermeable surfaces (impervious surface area) in the city of Fuzhou, capital of Fujian Province of China in 1989 and 2001 using Landsat TM and ETM+. Characteristics of the surface temperature of the urban area analyzed by knowing its links with the percentage of impervious surface area, NDVI values and NDBI. The results showed that the relationship between NDVI and LST weak, but there is a strong relationship between the ISA (sub-pixel Impervious Surface Area), NDBI, and LST. This study shows that the percentage of ISA, combined with LST and NDBI can quantitatively describe the spatial distribution and variation termporal urban heat patterns associated with the landcover condition.

Based on the study on the use of parameters NDBI from Landsat optical data, it can be seen that the parameter NDBI frequently used and a variable useful in understanding the condition of land cover, especially the undeveloped land, in urban and rural areas. In this study, these parameters will be attempted to be used for the detection of the locations of undeveloped land (settlements) in the rural areas, on the volcanic landform region, using the latest generation of optical data Landsat Landsat-8 OLI. This research aims to detect the spatial distribution of the settlement on volcanic region using Landsat-8 OLI imagery. Point of novelty of the study was not done research that seeks to detect the locations of special settlements in the area of the volcanic landforms NDBI based on parameters extracted from the Landsat-8 OLI.

2 METHODS

The study took place in the area of the volcanic landforms Sinabung Volcano, the Karo district of North Sumatra province. Volcano eruption is experienced in late 2013 and continued until the beginning of 2014. The eruption has caused a disaster with human casualties, and damage and destroy property, buildings, agricultural land and infrastructure (BNPB, 2013). Settlement areas are located on the slopes of the volcano has unique characteristics. First, the area is located on the slopes tend to be slanted or flat. Second, generally a rural settlement areas in the vicinity are surrounded by dense vegetation. Third, has a low density, even remote. Individually, of course the size of the area is in the collection has a relatively small size compared to settlements on the plain. This condition becomes interesting from the remote sensing, because it required a special detection method for object/area with these characteristics. In this study tested the use of the latest generation of Landsat imagery (Landsat-8) to detect the presence of the locations of settlements on the unique geographical conditions.

The data used is Landsat-8 OLI dated June 7, 2013 recording scene for a number of path/row 129/058. Radiometric correction performed to calculate the reflectance values. Delineation of volcanic landforms done visually with screen digitizing techniques (*onscreen digitation*). NDBI value is calculated by adopting the method of calculation of Zha *et al.* (2003). NDBI value is then used to separate classes of settlements with the thresholding method and the method of maximum likelihood supervised classification.

a. Radiometric Correction

Landsat-8 product offered by USGS EROS Data Center is the Digital Number quantized and calibrated including data recording results by sensors Operational Land Imager (OLI) and the Thermal Infrared Sensor (TIRS). This product is made in the format of 16-bit unsigned integer. This data can be scaled to the reflectance Top of Atmosphere (TOA) and/ or radians using rescaling using radiometric coefficients that have been available in the product file metadata (file MTL) . In addition, MTL file also contains a thermal constants needed for data conversion TIRS to the brightness temperature values (brightness temperature) (USGS, 2013).

Digital Number to Radiance Convertion

Data OLI and TIS can be converted to TOA spectral radiance using the following equation:

$$L_\lambda = M_L Q_{cal} + A_L \quad (2\text{-}1)$$

Where Lλ is TOA spectral radiance (Watts/ (m2 * srad * m)), ML is a band-specific additive rescaling factor derived from the file metadata (RADIANCE_ADD_BAND_x, where x is the number of band), AL is a band-specific additive rescaling factor obtained from file metadata (RADIANCE_ ADD_BAND_x, where x is the number of bands), as well as Qcal is Quantized and calibrated standard product pixel values (DN).

Convertion to TOA Reflectance

OLI data can also be converted to TOA planetary reflectance using the following equation:

$$\rho\lambda' = M_\rho Q_{cal} + A_\rho \quad (2\text{-}2)$$

Where ρλ 'is TOA planetary reflectance, without correction solar angle. Note that ρλ 'does not contain corrections sun angle, Mρ are band-specific multiplicative rescaling factor derived from the file metadata (REFLECTANCE_MULT_BAND_x, where x is the number of band), Aρ are band-

specific additive rescaling factor derived from the file metadata (REFLECTANCE_ ADD_BAND_x, where x is the number of band), and Qcal is Quantized and calibrated standard product pixel values (DN).

TOA reflectance with the sun angle correction, calculated by the following equation:

$$\rho\lambda = \frac{\rho\lambda'}{\cos(\theta_{SZ})} = \frac{\rho\lambda'}{\sin(\theta_{SE})} \quad (2\text{-}3)$$

Where ρλ is TOA planetary reflectance, θSE is Local sun elevation angle. Sun elevation angle at the center of the image scene in degrees is provided in the file metadata (SUN_ELEVATION), and θSZ is local solar zenith angle (θSZ = 90 ° - θSE). For a more accurate calculation of reflectance, solar angle per pixel can be used instead of Sun elevation angle at the center of the image scene. But the solar zenith angle of data per pixel are not currently provided with the product Landsat-8.

b. Delineation of Volcanic Landforms Region

Delineation of volcanic landforms Sinabung Volcano done visually in Landsat-8 OLI. To further refine the visual appearance of the image-making process is done 654 RGB color composite image is sharpened by the panchromatic channel (band 8) in order to obtain images with a spatial resolution of 15 meters. SRTM DEM data is 30 meter resolution is also used to display more clearly mountainous relief.

c. The calculation of the value of NDBI

Zha *et al.* (2003) developed a calculation of the value of the Landsat TM NDBI using the following equation:

$$NDBI = \frac{\rho 5 - \rho 4}{\rho 5 + \rho 4} \quad (2\text{-}24)$$

Where ρ5 and 4 respectively the reflectance channel 5 and channel 4.
Observing the spectral characteristics of the Landsat-8 OLI is different with Landsat TM. If want to apply the model equations NDBI using Landsat-8, then that should be examined is the spectral characteristics of the Landsat-8 OLI and the similarity or resemblance to Landsat-7 ETM +. Table 2-1 shows the comparison of spectral channels in the Landsat-7 ETM + and Landsat-8 OLI.

Table 2-1: Comparison of spectral channels in the Landsat-7 ETM + and Landsat-8 OLI

Sensor ETM+				Sensor OLI and TIRS			
Channel	Spectrum	Wave Length	Spatial Resolution	Channel	Spectrum	Wave Length	Spatial Resolution
				1	Visible	0.433 – 0.453	30 m
1	Visible	0.45 – 0.52	30 m	2	Visible	0.450 – 0.515	30 m
2	Visible	0.52 – 0.60	30 m	3	Visible	0.525 – 0.600	30 m
3	Visible	0.63 – 0.69	30 m	4	Visible	0.630 – 0.680	30 m
4	NIR	0.77 – 0.90	30 m	5	NIR	0.845 – 0.885	30 m
				9	Cirrus	1.360 – 1.390	30 m
5	NIR	1.55 – 1.75	30 m	6	SWIR	1.560 – 1.660	30 m
6	Thermal	10.40 – 12.50	60 m	10	TIRS 1	10.6 – 11.19	100 m
				11	TIRS 2	11.5 – 12.51	100 m
7	Mid-IR	2.08 – 2.35	30 m	7	SWIR	2.100 – 2.300	30 m
8	Panchromatic	0.52 – 0.90	15 m	8	Panchromatic	0.500 – 0.680	15 m

Noting the comparative characteristics of spectral channels in the Landsat-7 ETM + and Landsat-8 OLI, the equation for calculating NDBI 2-4 modified to be:

$$NDBI = \frac{\rho 6 - \rho 5}{\rho 6 + \rho 5} \quad (2\text{-}5)$$

$\rho 6$ and $\rho 5$ where respectively the reflectance channel 6 and channel 5 Landsat-8 OLI.

d. Extraction of settlement areas with thresholding method

Extraction of settlement areas is done with thresholding method. Several sample locations as a training area selected randomly to some location known as the location of settlements, based on its visual appearance, such as color, pattern, shape, association, size, and location. In determining the location of settlements training samples, created a composite image of natural color 6548 RGBI band combinations.

e. Accuracy Assesment

Accuracy test is done by comparing data extraction settlement with reference data. Data for reference data used visual delineation of settlements result of higher resolution imagery, in this study used Quickbird image. The degree of accuracy is calculated using the formula Individual Classification Success Index (ICSI) as follows (Koukoulas & Blackburn, 2001):

ICSI = 1 – Error of Omm % + Error of Comm % (2-6)

Explanation:

ICSI = *Individual Classification Success Index*

Omm = *Ommision;* class settlement entered into another class

Comm = *Commision;* additional settlement class from another class

3 RESULTS AND DISCUSSION

Results delineation of landforms visually on the Landsat-8 OLI color composite RGBI 6548 and combined with SRTM DEM data indicate that this type of shaped strato Sinabung volcano (stratovolcano) with an planimetric area of approximately 4,206 hectares. Figure 3-1 shows the Landsat-8 OLI color composite image with different views that show the form of a stratovolcano Sinabung.

NDBI value extraction results can be seen in Figure 3-2. Based on the extraction results characterizing NDBI value settlement areas on volcanic landforms. Selected training area of pixels that are considered settlements carried out visually on a composite image RGBI 6548. Examples of sample training area such settlements can be seen in Figure 4-3. Based on statistical calculations, the average value of the settlement is NDBI 0.108 with a standard deviation of 0.018. More clearly can be seen in Table 3-1.

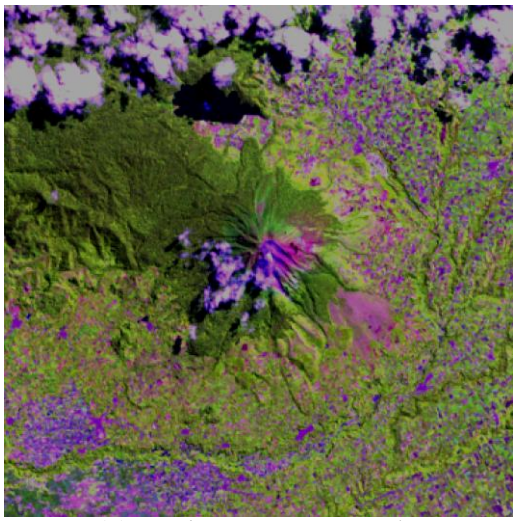

(a) Landsat-8 OLI RGB 654

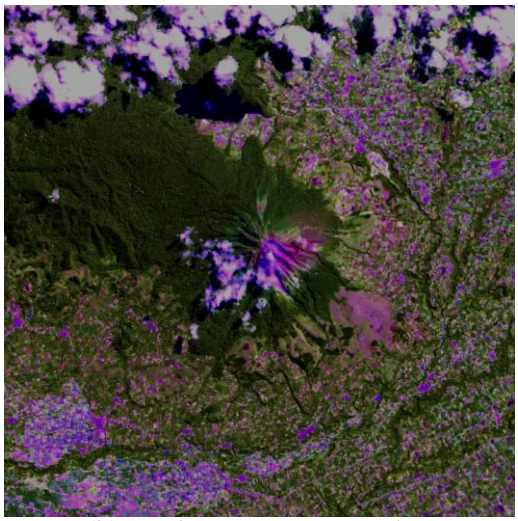

(b) Landsat-8 OLI RGBI 6548

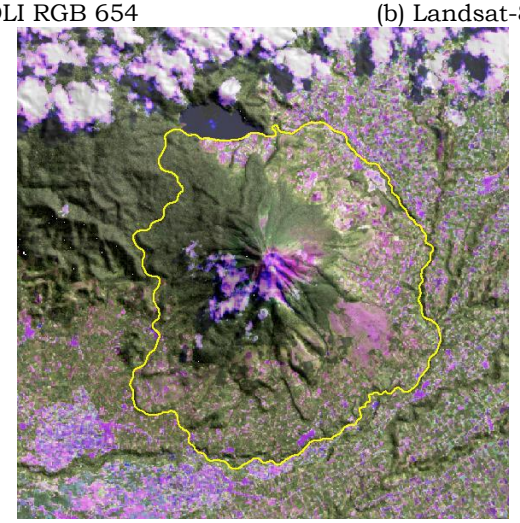

c) Landsat-8 OLI RGBI 6548 with background of DEM SRTM 30 m (transparancy 35%)

Figure 3-1: Landsat-8 OLI color composite image with different views that show the stratovolcano of Sinabung. Yellow line is the boundary of volcanic landforms

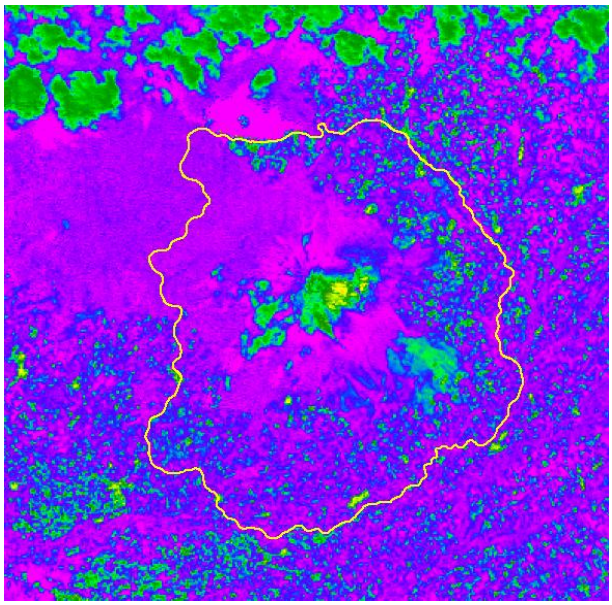

Figure 3-2: NDBI value Sinabung volcanic area. Yellow line is the boundary of volcanic landforms (unscale)

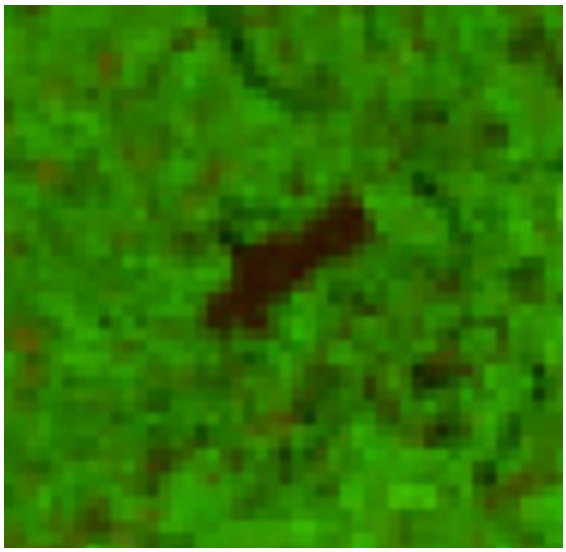

(a) Landsat-8 OLI RGB 654

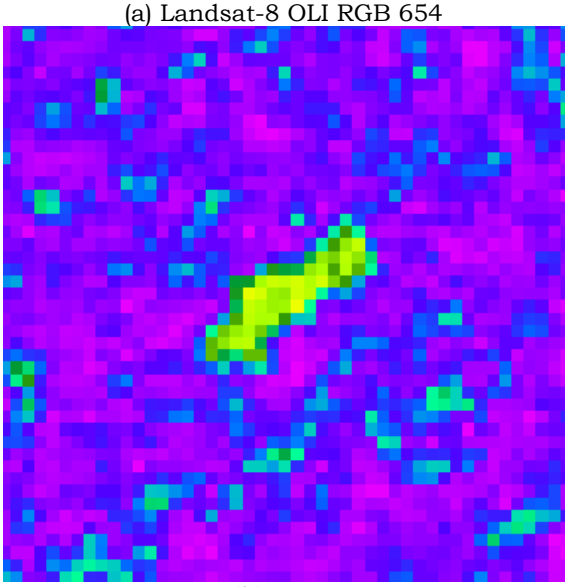

(b) NDBI

Figure 3-3: The zooming of the training settlement area located on the volcanic landform of Sinabung (unscale)

Extraction results pixels settlements with thresholding techniques (based on the mean and standard deviation of NDBI) is shown in Figure 3-4. Assuming a normal distribution then the specified threshold value of Mean ± 2StdDev. Based on the visible image can be seen in the distribution of settlement areas in Sinabung volcanic landforms. Based on identification, spatially, it can be seen that the spatial pattern of settlement in the volcanic landforms. In some locations already penetrated up to the slopes of the central part. Spatially, the distribution of settlements in Sinabung Volcano concentrated on the lower slopes and foot slopes of volcanoes. Scattered around the strato volcanoes in the north, northeast, east, southeast and south. In some locations there were settlements even in the south slope of the middle section.

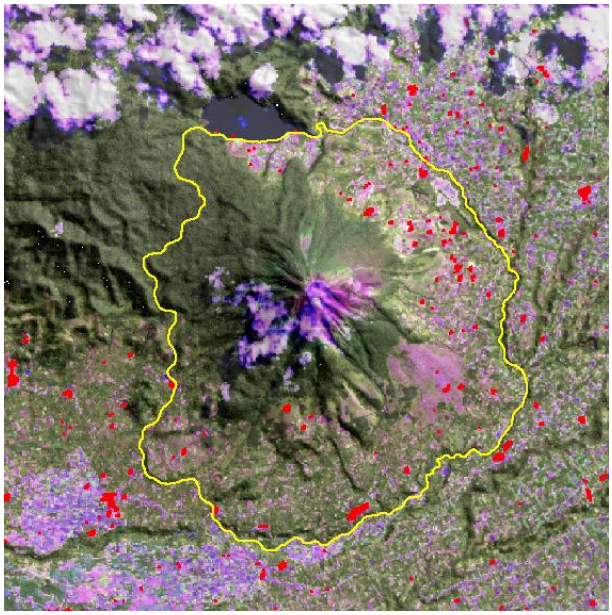

Figure 3-4: Teh result of extraction settlement area located on a volcanic landform of Sinabung using thresholding method based on the value NDBI

Table 3-1: NDBI value of various land cover in the region Sinabung Volcano

Landcover	Code	Min	Max	Mean	Std.Dev
Forests	F	-0.491	-0.406	-0.448	0.016
Shrublands	S	-0.200	-0.136	-0.165	0.012
Croplands	C	-0.483	-0.054	-0.322	0.087
Water	W	-0.697	-0.600	-0.641	0.018
Settlement - Volcan	St-V	0.087	0.158	0.108	0.018
Settlement - Non Volcan	St-nV	-0.039	0.119	0.049	0.035
Outcrops	OC	-0.169	-0.037	-0.105	0.044

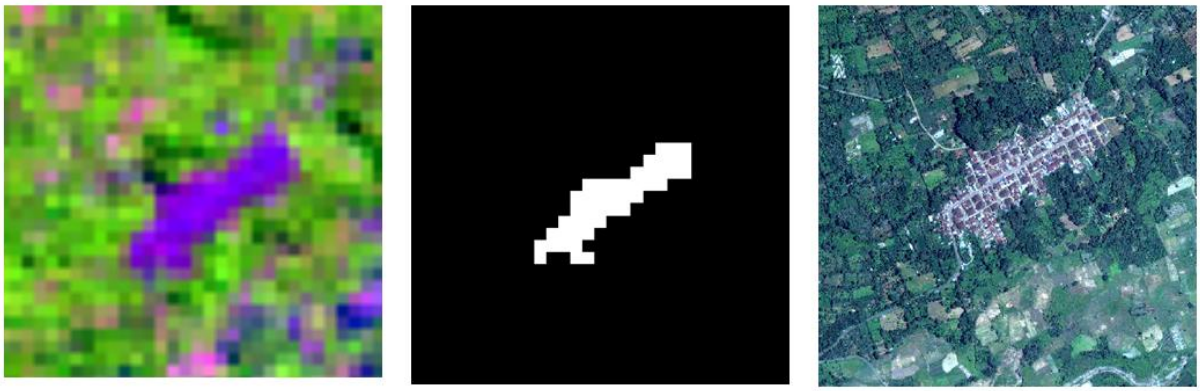

(a) Landsat-8 RGB 654 (b) Settlements resulted from extraction (c) Quickbird

Figure 3-5: Object appearance settlements in (a) Landsat-8 RGB 654, (b) Results of the extraction, and (c) Quickbird, 11 September 2010

The test results accuracy of identification results thresholding method using visual reference data delineation results from Quickbird image (11 September 2010) gives the results of the commision error of 36.90%, ommision error of 1.36%, and the value of the overall accuracy of 61.74%. Figure 3-5 shows the appearance of the object settlements in (a) Landsat-8 RGB 654, (b) Results of the extraction, and (c) Quickbird, 11 September 2010. Due to the condition of the region that has mountainous topography, it is to increase accuracy, that can be done is to make corrections reflectance due to the influence of topography (slope correction) (Richter *et al.*, 2009; Teillet *et al.* (1982)). It becomes the input for further research.

4 CONCLUSION

The study concluded that the spatial distribution of settlements on volcanic landforms can be identified easily and quickly from the Landsat-8 OLI based on the value NDBI using thresholding method. The spatial distribution of settlements in Sinabung Volcano concentrated on the lower slopes and foot slopes of volcanoes. Scattered around the strato volcanoes in the north, northeast, east, southeast and south. The mean value of the object NDBI settlements are relatively higher than other landcover object. In addition, the average value of the object NDBI settlements in volcanic higher than non-volcanic. The accuracy of test results showed that the use of this method gives quiet good results.

ACKNOWLEDGEMENT

This paper was part of a research program with the title “Pengembangan Model Pemanfaatan Penginderaan Jauh untuk Daerah Terkena Bencana Erupsi Gunung Api" (Model Development of the Application of Remote Sensing for Affected Area of the Volcanic Eruption) di Remote Sensing Application Center of LAPAN. The paper had previously been presented at the Seminar Nasional Penginderaan Jauh 2014 (National Seminar on Remote Sensing in 2014) under the title "Deteksi wilayah permukiman pada bentuklahan vulkanik menggunakan citra Landsat-8 OLI berdasarkan parameter Normalized Difference Build-up Index (NDBI)" (Detecting the settlement region on volcanic landform using Landsat-8 OLI based on parameter Normalized Difference Build-Up Index (NDBI)" and also was published in its proceedings. With some improvement and translation into English, then this paper finally published in this journal.

REFERENCES

As-syakur A., Adnyana IWS, Arthana IW, Nuarsa IW, (2012), Enhanced Built-Up and

Bareness Index (EBBI) for Mapping Built-Up and Bare Land in an Urban Area. Remote Sensing, 4:2957-2970.

Chen XL, Zhao HM, Li PX, Yin ZY, (2006), Remote sensing image-based analysis of the relationship between urban heat island and land use/cover changes. Remote Sensing of Environment, 104:133-146.

Jiang J., Zhou J., Wu H., Zhang H., Zhang L., Xu J., (2005), Land cover changes in the rural-urban interaction of Xi'an region using Landsat TM/ETM data. Journal of Geographical Sciences 15(4):423-430.

Koukoulas S., Blackburn GA, (2001), Introducing New Indices for Accuracy Evaluation of Classified Images Representing Semi-Nat ural Woodland Environments. Photogrammetric Engineering & Remote Sensing 67(4): 499-510.

Nasipuri P., Chatterjee A., (2009), A Quantitative Approach for Analyzing the Relationship between Urban Heat Islands and Land Cover. Remote Sensing (4):3596-3618.

Ogashawara I., Bastos VSB, (2012), A Quantitative Approach for Analyzing the Relationship between Urban Heat Islands and Land Cover. Remote Sensing 4:3596-3618.

Ritter FD, (1979), Process Geomorphology, Southern Illnuois Universityat Carbondale, Iowa: Brown Co. Publishers Duque.

Suwarsono, Khomarudin MR, (2014), Deteksi wilayah permukiman pada bentuklahan vulkanik menggunakan citra Landsat-8 OLI berdasarkan parameter Normalized Difference Build-up Index (NDBI). Prosiding Seminar Penginderaan Jauh 2014:345-356.

Thornbury WD, (1954), Principles of Geomorphology 2nded. New York: John Wiley & Sons, Inc.

Uddin S., Al Ghadban AN, Al Dousari A., Al Murad M., Al Shamroukh, (2010), A remote sensing classification for land-cover changes and micro-climate in Kuwait. International Journal of Sustainable Development Planning: 1-11.

USGS,http://landsat.usgs.gov/Landsat8_Using_ Product.php,diakses pada 2013-06-01 jam 03:48 pm.

Xu H., Huang S., Zhang T., (2013), Built-up land mapping capabilities of the ASTER and Landsat ETM+ sensors in coastal areas of southeastern China. Advances in Space Research 52:1437-1449.

Zha Y., Gao J., Ni S., (2003), Use of normalized difference built-up index in automatically mapping urban areas from TM imagery. International Journal of Remote Sensing, 24(3): 583–594.

Zhang H., Du P., Luo Y., Liu P., (2008), Analysis of Relationship between Urban Thermal Pattern and Land Use/Land Cover-Taking Xuzhou City as an Example. Proceedings of Information Technology and Environmental System Sciences:1058-1062.

Zhang Y., Odeh LAO, Han C., (2009), Bi-temporal characterization of land surface temperature in relation to impervious surface area, NDVI and NDBI, using a sub-pixel image analysis. International Journal of Applied Earth Observation and Geoinformation 11:256-264.

Zuidam RAV, (1985), Aerial Photo-Interpretationin Terrain Analysis and Geomorphologic Mapping, ITC Enschede, The Netherlands.